

Supplementary Materials

Understanding the Reactivity of Trimethylsilyldiazoalkanes Participating in [3+2] Cycloaddition Reactions towards Diethylfumarate with a Molecular Electron Density Theory Perspective

Luis R. Domingo ^{1,*}, Nivedita Acharjee ^{2,*} and Haydar A Mohammad-Salim ³

¹ Department of Organic Chemistry, University of Valencia, Dr. Moliner 50, Burjassot, E-46100 Valencia, Spain

² Department of Chemistry, Durgapur Government College, Durgapur-713214, West Bengal, India

³ Department of Chemistry, University of Zakho, Duhok 42001, Iraq; hayder.salim@uoz.edu.krd

* Correspondence: domingo@utopia.uv.es (L.R.D.); nivchem@gmail.com (N.A.); Tel.: +0-947-415-0273 (N.A.)

Index

S2 1. BET study of the 32CA reaction of TSDE 1 with DFM 4.

S4 2. BET study of the 32CA reaction of TSDA 3 with DFM 4.

S6 References.

S7 Table with the MPWB1K/6-311G(d,p) calculated gas phase total energies, enthalpies, and Gibbs free energies, computed at 298 K, of the stationary points involved in the 32CA reactions of TSDE 1, TSDP 2 and TSDA 3, with DFM 4.

S8 Table with the MPWB1K/6-311G(d,p) calculated total energies, enthalpies, and Gibbs free energies, computed at 298 K in carbon tetrachloride, of the stationary points involved in the 32CA reactions of TSDE 1, TSDP 2 and TSDA 3, with DFM 4.

1. BET study of the 32CA reaction of TSDE 1 with DFM 4

The Bonding Evolution Theory¹ (BET), which comes from the conjunction of the electron localization function^{2,3} (ELF) topological analysis and the Thom's Catastrophe theory,⁴ has proven to be a very useful methodological tool to establish the nature of the electronic rearrangement taking place along the reaction path.⁵ Herein, the BET of the 32CA reaction of TSDE 1 with DFM 4 is first studied. The populations of the most significant valence basins, among other relevant parameters, are given in Table S1.

The 32CA reaction of TSDE 1 with DFM 4 takes place along nine different phases (see Table S1). *Phase I* begins at the structure **S1-I**, $d_{N1-C5} = 2.55 \text{ \AA}$ and $d_{C3-C4} = 2.60 \text{ \AA}$, which is the starting structure of the IRC of this 32CA reaction. ELF of **S1-I** is very similar to that of the separated reagents (see Section 3.1). The only difference being in the total integrating population of the $V(N1,N2)$ and $V'(N1,N2)$ disynaptic basins, 3.69 e in TSDE 1 and 3.61 e in **S1-I**, while the population of the $V(C3,N2)$ disynaptic basin in TSDE 1 and **S1-I** are 3.07 e and 3.28 e, respectively, suggesting the changes in electronic distribution of the N1-N2-C3 moiety with the change in geometry from TSDE 1 to the starting IRC point **S1-I**. Note that **S1-I** shows a GEDT of 0.16 e, fluxing from the trimethylsilyldiazoalkane framework to the DFM one, owing to the strong nucleophilic character of TSDE 1 and strong electrophilic character of DFM 4. (see Section 3.2).

Phase II starts at the structure **S2-I**, $d_{N1-C5} = 2.43 \text{ \AA}$ and $d_{C3-C4} = 2.47 \text{ \AA}$, with an energy cost (EC) of 2.4 kcal·mol⁻¹ and a GEDT of 0.20 e. At **S2-I**, the two $V(C4,C5)$ and $V'(C4,C5)$ disynaptic basins have merged into one $V(C4,C5)$ disynaptic basin integrating at 3.19 e, suggesting an EC of 2.4 kcal·mol⁻¹ for the rupture of C4-C5 double bond of DFM 4 along the reaction path.

Phase III starts at the structure **S3-I**, $d_{N1-C5} = 2.30 \text{ \AA}$ and $d_{C3-C4} = 2.32 \text{ \AA}$, with an EC of 5.8 kcal·mol⁻¹ and a GEDT of 0.24 e. **S3-I** is associated with the formation of a new $V(N2)$ monosynaptic basin, integrating 1.22 e. The electron density demanded for the formation of this monosynaptic basin comes from the C3-N2 bonding region, which has been depopulated by 1.00 e, and also from the N1-N2 bonding region, which has experienced a depopulation of 0.18 e. This $V(N2)$ monosynaptic basin, which is associated with the lone pair present at the N2 nitrogen, experiences a continuous increase of its population until reach 2.65 e at pyrazole 6 at the end of the IRC.

Phase IV starts at the structure **S4-I**, $d_{N1-C5} = 2.26 \text{ \AA}$ and $d_{C3-C4} = 2.27 \text{ \AA}$, with an EC of 6.7 kcal·mol⁻¹. **S4-I** is characterized by the formation of a new $V(C3)$ monosynaptic basin integrating 0.54 e. The electron density demanded for the formation of this monosynaptic basin comes from the depopulation of the C3-N2 bonding region, which has been depopulated by 0.19 e. **S4-I** shows a GEDT value of 0.25 e.

Phase V starts at the structure **S5-I**, $d_{N1-C5} = 2.18 \text{ \AA}$ and $d_{C3-C4} = 2.17 \text{ \AA}$, with an EC of 7.6 kcal·mol⁻¹. **S5-I** is characterized by the formation of a new $V(C4)$ monosynaptic basin, integrating 0.18 e, which is formed by deriving electron density from the C4-C5 bonding region, which experiences a depopulation of 0.17 e. **TS2** belongs to Phase IV. This suggests that the activation energy of this 32CA reaction is mainly associated with the EC demanded for the formation of the *pseudoradical*⁶ C3 and C4 carbons at the interacting nuclei, and for the formation of the non-bonding electron density at the N2 nitrogen, which demand the depopulation of the N2-C3 and C4-C5 bonding regions. **S5-I** shows a GEDT value of 0.26 e, suggesting a polar reaction.

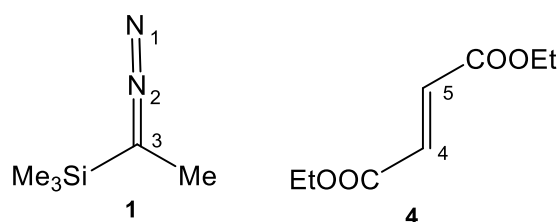
Phase VI starts at the structure **S6-I**, $d_{N1-C5} = 2.09 \text{ \AA}$ and $d_{C3-C4} = 2.06 \text{ \AA}$, which is characterized by the formation of a new $V(C5)$ monosynaptic basin, integrating 0.19 e. The electron density demanded for the creation of this monosynaptic basin comes from the depopulation of the C4-C5 bonding region that has been depopulated by 0.32 e. At **S6-I** the populations of the $V(C3)$ and $V(C4)$ monosynaptic basins have been increased by 0.70 and 0.36 e, respectively.

Phase VII starts at the structure **S7-I**, $d_{N1-C5} = 2.01 \text{ \AA}$ and $d_{C3-C4} = 1.96 \text{ \AA}$. At the beginning of this phase, the first more relevant change along the IRC takes place. At this structure, while the $V(C4)$ and $V(C3)$ monosynaptic basin present at **S6-I** are missing, a new $V(C3,C4)$ disynaptic basin, integrating 1.26 e, is created. These topological changes indicate that the formation of the first C3-C4 single bond takes place at a C3-C4 distance of 1.96 Å by the C-to-C coupling of the two *pseudoradical* C3 and C4 carbons.⁷

Phase VIII starts at the structure **S8-I**, $d_{N1-C5} = 1.92 \text{ \AA}$ and $d_{C3-C4} = 1.86 \text{ \AA}$, which is characterized by the splitting of the $V(N1)$ monosynaptic basin into two monosynaptic basins $V(N1)$ and $V'(N1)$, respectively integrating 3.11 e and 0.52 e.

Finally, the last *Phase IX* starts at the structure **S9-I**, $d_{N1-C5} = 1.77 \text{ \AA}$ and $d_{C3-C4} = 1.73 \text{ \AA}$ and ends at pyrazole **6**. At **S9-I**, the second more relevant change along the IRC takes place. At this structure, while the $V(C5)$ and $V'(N1)$ monosynaptic basins are missing, a new $V(N1,C5)$ disynaptic basin, integrating 1.32, is created. These relevant topological changes indicate that the formation of the second N1-C5 single bond has begun at a C-N distance of 1.77 \AA through the C-to-N coupling of the electron density of the *pseudoradical* C5 carbon present at **S8-I** and part of the non-bonding electron density of the N1 nitrogen. Along this last phase, the molecular electron density is relaxed to reach the structure of pyrazole **6**, in which the $V(C3,C4)$ and $V(N1,C5)$ disynaptic basins reach a population of 1.84 and 1.75 e, respectively (see Table S1).

Table 1. ELF valence basin populations, distances of the forming bonds, and relative^a electronic energies of the IRC structures **S1-I** – **S9-I** defining the nine phases characterizing the molecular mechanism of the 32CA reaction of TSDE **1** and DFM **4**. Distances are given in angstroms, \AA , and relative energies in $\text{kcal}\cdot\text{mol}^{-1}$.



Phases	I	II	III	IV	V	VI	VII	VIII	IX	
Structures	S1-I	S2-I	S3-I	S4-I	S5-I	S6-I	S7-I	S8-I	S9-I	6
$d(N1-C5)$	2.55	2.43	2.30	2.26	2.18	2.09	2.01	1.92	1.77	1.48
$d(C3-C4)$	2.60	2.47	2.32	2.27	2.17	2.06	1.96	1.86	1.73	1.55
ΔE	0.0	2.4	5.8	6.7	7.6	6.5	2.9	-3.1	-14.3	-32.3
GEDT	0.16	0.20	0.24	0.25	0.26	0.25	0.21	0.16	0.07	0.04
$V(N1)$	3.73	3.70	3.63	3.62	3.60	3.59	3.59	3.11	2.90	2.75
$V'(N1)$								0.52		
$V(N1,N2)$	1.88	1.84	1.78	1.73	1.67	1.62	2.89	2.80	2.69	2.54
$V'(N1,N2)$	1.73	1.66	1.54	1.51	1.44	1.37				
$V(C3,N2)$	3.28	3.42	2.42	2.23	2.07	2.00	1.94	1.91	1.89	1.84
$V(N2)$			1.22	1.50	1.82	2.05	2.23	2.36	2.51	2.65
$V(C4,C5)$	1.76	3.19	3.14	3.13	2.96	2.64	2.43	2.27	2.12	1.97
$V'(C4,C5)$	1.46									
$V(C3,C6)$	1.90	1.91	1.92	1.92	1.92	1.91	1.90	1.89	1.88	1.87
$V(C3)$				0.54	0.63	0.70				
$V(C4)$					0.18	0.36				
$V(C5)$						0.19	0.33	0.43		
$V(C3,C4)$							1.26	1.42	1.60	1.84
$V(N1,C5)$									1.32	1.75

2. BET study of the 32CA reaction of TSDA 3 with DFM 4

Herein, the BET of the 32CA reaction of TSDA 3 with DFM 4 is studied. The populations of the most significant valence basins, among other relevant parameters, are given in Table S2.

The 32CA reaction of TSDA 3 with DFM 4 takes place along nine different phases (see Table S1). *Phase I* begins at the structure **S1-II**, $d_{N1-C5} = 2.71 \text{ \AA}$ and $d_{C3-C4} = 2.74 \text{ \AA}$, which is the starting structure of the IRC of this 32CA reaction. ELF of **S1-II** is very similar to that of the separated reagents (see Section 3.1). The only difference being in the total integrating population of the $V(N1,N2)$ and $V'(N1,N2)$ disynaptic basins, 3.86 e at TSDA 3 and 3.81 e at **S1-II**, while the population of the $V(C3,N2)$ disynaptic basin is 2.93 e and 3.04 e at TSDA 3 and **S1-II**, respectively, suggesting the changes in electronic distribution of the $N1-N2-C3$ moiety with the in geometry at the starting IRC point **S1-II**. Note that **S1-II** shows a GEDT of 0.08 e, fluxing from the trimethylsilyldiazoalkane framework to the DFM one, which is less than that at **S1-I** (see Table S1), as a consequence of the moderate nucleophilic character of TSDA 3 (see Section 3.2.)

Phase II starts at the structure **S2-II**, $d_{N1-C5} = 2.36 \text{ \AA}$ and $d_{C3-C4} = 2.38 \text{ \AA}$, with an EC of 9.4 kcal·mol⁻¹ and GEDT of 0.17 e. At **S2-II**, the two $V(C4,C5)$ and $V'(C4,C5)$ disynaptic basins have merged into one $V(C4,C5)$ disynaptic basin, integrating at 3.17 e, suggesting an EC of 9.4 kcal·mol⁻¹ for the rupture of $C4-C5$ double bond of DFM 4 along the reaction path. Note that the EC for the rupture of $C4-C5$ bond of DFM 4 is 2.4 kcal mol⁻¹ for 32CA reaction with TSDE 1, while the EC is 9.4 kcal mol⁻¹ for 32CA reaction with 3, which suggests that increase in GEDT causes less EC demand, resulting in the easy rupture of the C-C double bond.⁸

Phase III starts at the structure **S3-II**, $d_{N1-C5} = 2.22 \text{ \AA}$ and $d_{C3-C4} = 2.22 \text{ \AA}$, with an EC of 14.2 kcal·mol⁻¹ and GEDT of 0.19 e. **S3-II** is associated with the formation of a new $V(N2)$ monosynaptic basin, integrating at 1.52 e. The electron density demanded for formation of this monosynaptic basin comes from of the $C3-N2$ bonding region, which has been depopulated by 1.20 e, and also from the $N1-N2$ bonding region, which has experienced depopulation of 0.27 e. This $V(N2)$ monosynaptic basin, which is associated with the lone pair present at the $N2$ nitrogen, experiences a continuous increase of its population until reach 2.65 e at pyrazole 10 at the end of the IRC.

Phase IV starts at the structure **S4-II**, $d_{N1-C5} = 2.17 \text{ \AA}$ and $d_{C3-C4} = 2.16 \text{ \AA}$, with an EC of 15.2 kcal·mol⁻¹. **S4-II** is characterized by the formation of a new $V(C3)$ monosynaptic basin integrating 0.55 e. The electron density demanded for the formation of this monosynaptic basin comes from the depopulation of the $C3-N2$ bonding region, which has been depopulated by 0.09 e. **S4-I** shows a GEDT value of 0.19 e.

Phase V starts at the structure **S5-II**, $d_{N1-C5} = 2.13 \text{ \AA}$ and $d_{C3-C4} = 2.11 \text{ \AA}$, with an EC of 15.5 kcal·mol⁻¹. **S5-II** is characterized by the formation of a new $V(C4)$ monosynaptic basin, integrating 0.20 e, which is formed by deriving electron density from the $C4-C5$ bonding region, which experiences a depopulation of 0.19 e. **TS6** belongs to Phase IV. This suggests that the activation energy of this 32CA reaction is mainly associated with the EC demanded for the formation of the pseudoradical⁶ $C3$ and $C4$ carbons at the interacting nuclei, and for the formation of the non-bonding electron density at the $N2$ nitrogen, which demands the previous depopulation of the $C3-N2$ and $C4-C5$ bonding regions. **S5-I** shows a GEDT value of 0.19 e, suggesting a less polar reaction compared to the 32CA reaction of TSDE 1 with DFM 4 (see Table S1).

Phase VI starts at the structure **S6-II**, $d_{N1-C5} = 2.08 \text{ \AA}$ and $d_{C3-C4} = 2.06 \text{ \AA}$, which is characterized by the formation of a new $V(C5)$ monosynaptic basin, integrating 0.17 e. The electron density demanded for the creation of this monosynaptic basin comes from the depopulation of the $C4-C5$ bonding region that has been depopulated by 0.23 e. At **S6-II**, the populations of the $V(C3)$ and $V(C4)$ monosynaptic basins have been increased by 0.68 and 0.29 e, respectively.

Phase VII starts at the structure **S7-II**, $d_{N1-C5} = 2.03 \text{ \AA}$ and $d_{C3-C4} = 2.00 \text{ \AA}$. At the beginning of this phase the first more relevant change along the IRC takes place. At this structure, while the $V(C4)$ and $V(C3)$ monosynaptic basin present at **S6-II** are missing, a new $V(C3,C4)$ disynaptic basin, integrating 1.10 e, is created. These topological changes indicate that the formation of the first $C3-$

C4 single bond takes place at a C3-C4 distance of 2.00 Å by the C-to-C coupling of the *pseudoradical* C3 and C4 carbons.⁷

Phase VIII starts at the structure **S8-II**, $d_{N1-C5} = 1.89$ Å and $d_{C3-C4} = 1.84$ Å, which is characterized by the splitting of the V(N1) monosynaptic basin into two monosynaptic basins, V(N1) and V'(N1), integrating 2.99 e and 0.61 e, respectively.

Finally, the last *Phase IX* starts at the structure **S9-II**, $d_{N1-C5} = 1.78$ Å and $d_{C3-C4} = 1.74$ Å and ends at pyrazole **10**. At **S9-II**, the second more relevant change along the IRC takes place. At this structure, while the V(C5) and V'(N1) monosynaptic basins are missing, a new V(N1,C5) disynaptic basin, integrating 1.30, is created. These relevant topological changes indicate that the formation of the second N1-C5 single bond has begun at a C-N distance of 1.78 Å through the C-to-N coupling of the electron density of the *pseudoradical* C5 carbon present at **S8-II** and part of the non-bonding electron density of the N1 nitrogen. Along this last phase, the molecular electron density is relaxed to reach the structure of pyrazole **10**, in which the V(C3,C4) and V(N1,C5) disynaptic basins reach a population of 1.83 and 1.76 e, respectively (see Table S2).

Table 2. ELF valence basin populations, distances of the forming bonds, and relative^a electronic energies of the IRC structures **S1-II** – **S9-II** defining the nine phases characterizing the molecular mechanism of the 32CA reaction of TSDA **3** and DFM **4**. Distances are given in angstroms, Å, and relative energies in kcal·mol⁻¹.



Phases	I	II	III	IV	V	VI	VII	VIII	IX	
Structures	S1-II	S2-II	S3-II	S4-II	S5-II	S6-II	S7-II	S8-II	S9-II	10
d(N1-C5)	2.71	2.36	2.22	2.17	2.13	2.08	2.03	1.89	1.78	1.48
d(C3-C4)	2.74	2.38	2.22	2.16	2.11	2.06	2.00	1.84	1.74	1.55
ΔE	0.0	9.4	14.2	15.2	15.5	15.1	13.8	5.7	-2.0	-21.4
GEDT	0.08	0.17	0.19	0.19	0.19	0.18	0.17	0.10	0.04	0.07
V(N1)	3.60	3.54	3.51	3.51	3.52	3.52	3.54	2.99	2.88	2.74
V'(N1)								0.61		
V(N1,N2)	1.93	1.74	1.62	1.58	1.55	1.52	1.48	1.40	2.73	2.55
V'(N1,N2)	1.88	1.80	1.65	1.60	1.55	1.51	1.48	1.40		
V(C3,N2)	3.04	3.38	2.18	2.09	2.03	1.99	1.97	1.91	1.89	1.83
V(N2)			1.52	1.72	1.88	2.01	2.12	2.37	2.48	2.65
V(C4,C5)	1.75	3.17	3.10	3.10	2.91	2.68	2.54	2.20	2.14	1.95
V'(C4,C5)	1.51									
V(C3,C6)	2.37	2.37	2.33	2.31	2.30	2.28	2.26	2.25	2.20	2.17
V(C3)				0.55	0.62	0.68				
V(C4)					0.20	0.29				
V(C5)						0.17	0.26	0.44		
V(C3,C4)							1.10	1.39	1.54	1.83
V(N1,C5)									1.30	1.76

References

1. Krokidis, X.; Noury, S.; Silvi, B. Characterization of elementary chemical processes by Catastrophe Theory. *J. Phys. Chem. A* **1997**, *101*, 7277–7282, doi:10.1021/jp9711508.
2. Becke, A.D.; Edgecombe, K.E. A simple measure of electron localization in atomic and molecular systems. *J. Chem. Phys.* **1990**, *92*, 5397–5403, doi:10.1063/1.458517.
3. Silvi, B.; Savin, A. Classification of chemical bonds based on topological analysis of electron localization functions. *Nature*, **1994**, *371*, 683–686, doi:10.1038/371683a0.
4. (a) Thom, R. *Stabilité Structurelle et Morphogénèse*; Intereditions, Paris, 1972; (b) A. E. R. Woodcock, T. A. Poston in *Geometrical Study of Elementary Catastrophes*; Springer-Verlag, Berlin, 1974.
5. (a) Polo, V.; Andrés, J.; Berski, S.; Domingo, L. R.; Silvi, B. Understanding Reaction Mechanisms in Organic Chemistry from Catastrophe Theory Applied to the Electron Localization Function Topology. *J. Phys. Chem. A* **2008**, *112*, 7128–7136, doi:10.1021/jp801429m. (b) Andrés, J.; González-Navarrete, P.; Safont, V. Unraveling reaction mechanisms by means of Quantum Chemical Topology Analysis. *Int. J. Quantum Chem.* **2014**, *114*, 1239–1252, doi:10.1002/qua.24665. (c) Andrés, J.; Berski, S.; Domingo, L. R.; Polo, V.; Silvi, B. Describing the Molecular Mechanism of Organic Reactions by Using Topological Analysis of Electronic Localization Function. *Curr. Org. Chem.* **2011**, *15*, 3566–3575, doi:10.2174/138527211797636156.
6. (a) Domingo, L.R.; Chamorro, E.; Pérez, P. Understanding the High Reactivity of the Azomethine Ylides in [3 + 2] Cycloaddition Reactions. *Lett. Org. Chem.* **2010**, *7*, 432–439, doi:10.2174/157017810791824900. (b) Domingo, L.R.; Sáez, J. A. Understanding the Electronic Reorganization along the Nonpolar [3 + 2] Cycloaddition Reactions of Carbonyl Ylides. *J. Org. Chem.* **2011**, *76*, 373–379, doi:10.1021/jo101367v.
7. Domingo, L.R. A new C–C bond formation model based on the quantum chemical topology of electron density. *RSC Adv.* **2014**, *4*, 32415–32428, doi:10.1039/C4RA04280H.
8. Domingo, L.R.; Ríos-Gutiérrez, M.; Pérez, P. How does the global electron density transfer diminish activation energies in polar cycloaddition reactions? A Molecular Electron Density Theory study. *Tetrahedron*, **2017**, *73*, 1718–1724, doi:10.1016/j.tet.2017.02.012.

Table 3. MPWB1K/6-311G(d,p) calculated gas phase total energies, E, enthalpies, H, and Gibbs free energies, G in a.u, computed at 298K, of the stationary points involved in the 32CA reactions of TSDE 1, TSDP 2 and TSDA 3, with DFM 4.

	E	G	H
1	-596.675399	-596.547380	-596.495537
2	-788.369446	-788.190175	-788.131818
3	-824.53065	-824.361063	-824.301465
4	-612.839476	-612.678978	-612.624071
TS1	-1209.499856	-1209.181955	-1209.103068
5	-1209.566566	-1209.244156	-1209.166528
TS2	-1209.502710	-1209.186709	-1209.106633
6	-1209.566281	-1209.247477	-1209.166698
TS3	-1401.186568	-1400.821434	-1400.732903
7	-1401.253526	-1400.882224	-1400.797095
TS4	-1401.1909130	-1400.826655	-1400.738747
8	-1401.249970	-1400.878496	-1400.795056
TS5	-1437.340483	-1436.985155	-1436.895283
9	-1437.402467	-1437.04474	-1436.953811
TS6	-1437.345212	-1436.989932	-1436.901317
10	-1437.404242	-1437.045646	-1436.956793

Table 4. MPWB1K/6-311G(d,p) calculated total energies, E, enthalpies, H, and Gibbs free energies, G in a.u., computed at 298 K in carbon tetrachloride, of the stationary points involved in the 32CA reactions of TSDE 1, TSDP 2 and TSDA 3, with DFM 4.

	E	G	H
1	-596.676758	-596.549095	-596.497121
2	-788.371550	-788.192339	-788.13409
3	-824.532823	-824.363670	-824.303954
4	-612.843051	-612.683006	-612.627833
TS1	-1209.504272	-1209.189376	-1209.108587
5	-1209.571556	-1209.249562	-1209.171773
TS2	-1209.507631	-1209.19292	-1209.112259
6	-1209.571474	-1209.253204	-1209.172217
TS3	-1401.191540	-1400.82696	-1400.73848
7	-1401.258189	-1400.888044	-1400.802444
TS4	-1401.196052	-1400.831071	-1400.743128
8	-1401.255517	-1400.884444	-1400.801023
TS5	-1437.345050	-1436.991129	-1436.900375
9	-1437.408552	-1437.051554	-1436.960381
TS6	-1437.349804	-1436.996108	-1436.905429
10	-1437.410323	-1437.051978	-1436.963283